Research Article

MOLECULAR PAIN

Molecular Pain
Volume 14: 1–15

DOI: 10.1177/1744806918776467
journals.sagepub.com/home/mpx
SAGE

Functional effects of TrkA inhibition on system x_C^--mediated glutamate release and cancer-induced bone pain

Tanya Miladinovic[1,2], Robert G Ungard[1,2], Katja Linher-Melville[1,2], Snezana Popovic[2] and Gurmit Singh[1,2]

Abstract

Breast cancer cells release the signalling molecule glutamate via the system x_C^- antiporter, which is upregulated to exchange extracellular cystine for intracellular glutamate to protect against oxidative stress. Here, we demonstrate that this antiporter is functionally influenced by the actions of the neurotrophin nerve growth factor on its cognate receptor tyrosine kinase, TrkA, and that inhibiting this complex may reduce cancer-induced bone pain via its downstream actions on xCT, the functional subunit of system x_C^-. We have characterized the effects of the selective TrkA inhibitor AG879 on system x_C^- activity in murine 4T1 and human MDA-MB-231 mammary carcinoma cells, as well as its effects on nociception in our validated immunocompetent mouse model of cancer-induced bone pain, in which BALB/c mice are intrafemorally inoculated with 4T1 murine carcinoma cells. AG879 decreased functional system x_C^- activity, as measured by cystine uptake and glutamate release, and inhibited nociceptive and physiologically relevant responses in tumour-bearing animals. Cumulatively, these data suggest that the activation of TrkA by nerve growth factor may have functional implications on system x_C^--mediated cancer pain. System x_C^--mediated TrkA activation therefore presents a promising target for therapeutic intervention in cancer pain treatment.

Keywords

Cancer, pain, system x_C^-, glutamate, neurotrophin, nerve growth factor

Date Received: 16 January 2018; revised: 26 March 2018; accepted: 5 April 2018

Introduction

Breast cancer has a propensity to metastasize to the bone, causing severe cancer-induced bone pain (CIBP) and reduced quality of life. Accordingly, the effective management of CIBP is essential to improving quality of life for cancer patients. Our group has demonstrated that breast cancer cells secrete the signalling molecule glutamate via system x_C^- and overexpress the gene encoding this antiporter.[1,2] When glutamate efflux becomes excessive, its character within the central nervous system switches from an excitatory transmitter to a well-characterized and pathologically relevant excitotoxin.[3,4] Considerable evidence suggests that glutamate released through system x_C^- is involved in multiple physiological and pathological processes (Reviewed in Miladinovic et al.[5]). Its dysregulation has been linked to chronic pain, an effect which is supported by animal models of CIBP.[6,7] Exogenous glutamate released from peripheral metastases may then sensitize surrounding nerves, directly acting on adjacent nociceptors within the bone environment.

The neurotrophin nerve growth factor (NGF) acts via its cognate receptor TrkA, through which it activates several downstream signalling pathways that regulate neuronal survival and differentiation. While normal breast epithelial tissue does not rely on NGF-TrkA

[1]Michael G. DeGroote Institute for Pain Research and Care, McMaster University, Hamilton, Ontario, Canada
[2]Department of Pathology and Molecular Medicine, McMaster University, Hamilton, Ontario, Canada

Corresponding Author:
Gurmit Singh, Department of Pathology and Molecular Medicine, McMaster University, 1280 Main Street West, Hamilton, Ontario, Canada L8N 3Z5.
Email: singhg@mcmaster.ca

signalling, breast cancer cells express the TrkA receptor,[8,9] and NGF is a potent activator of the survival and proliferation of breast cancer cells.[8] Furthermore, biologically active NGF is excessively synthesized and released by breast cancer cells, an effect which is blocked by the TrkA inhibitor K252, indicating the existence of an NGF autocrine loop.[10]

In humans, endogenous NGF levels are elevated in pain states associated with chronic conditions,[11–14] and NGF appears to be an important driver of the increased pain sensitivity characteristic of late stage metastatic cancer (reviewed in Wang et al.[15]). Correspondingly, in animal models of nociception, NGF- and TrkA-knockout mice are hypoalgesic,[16,17] while transgenic animals that overexpress NGF exhibit hyperalgesic behaviours.[18,19] Preclinical research suggests that anti-NGF treatment may be particularly effective in pain that originates in bone,[20–25] as more than half of the nerve fibres that innervate bone are responsive to NGF.[26]

To date, research on the neurotrophic consequences of metastatic cancer has largely focused on pathological nerve sprouting of sensory and sympathetic nerve fibres that innervate the tumour-bearing host tissue.[20,24,27,28] Below, we propose an alternative consideration and complementary explanation of the role of NGF-TrkA in CIBP (See Figure 1 for schematic).

There is considerable evidence for bidirectional signalling between glutamate and neurotrophins. Glutamate stimulates neurotrophic expression,[29,30] and the neurotrophin fibroblast growth factor-2 has been implicated in the functional upregulation of system x_C^- in mixed neuronal and glial cultures.[31] Glutamate plays a key role in several neurodevelopmental and neurodegenerative disorders, and overexpression of system x_C^- has been shown to have neuroprotective effects in conditions of oxidative stress.[32] Furthermore, NGF,[10] TrkA[33] and xCT[1,2] are upregulated in breast cancer cells, supporting the notion that a functional relationship exists. The overlapping actions of xCT and NGF suggest that system x_C^- may be influenced by neurotrophic activity. To further elucidate the underlying pathophysiology of glutamate-related cancer pain, we have focused on the NGF-TrkA complex as a therapeutic target to reduce aberrant system x_C^--meditated glutamate release that accompanies CIBP. Here, we test the hypothesis that systematically inhibiting the actions of NGF on TrkA may reduce CIBP by decreasing functional system x_C^- activity.

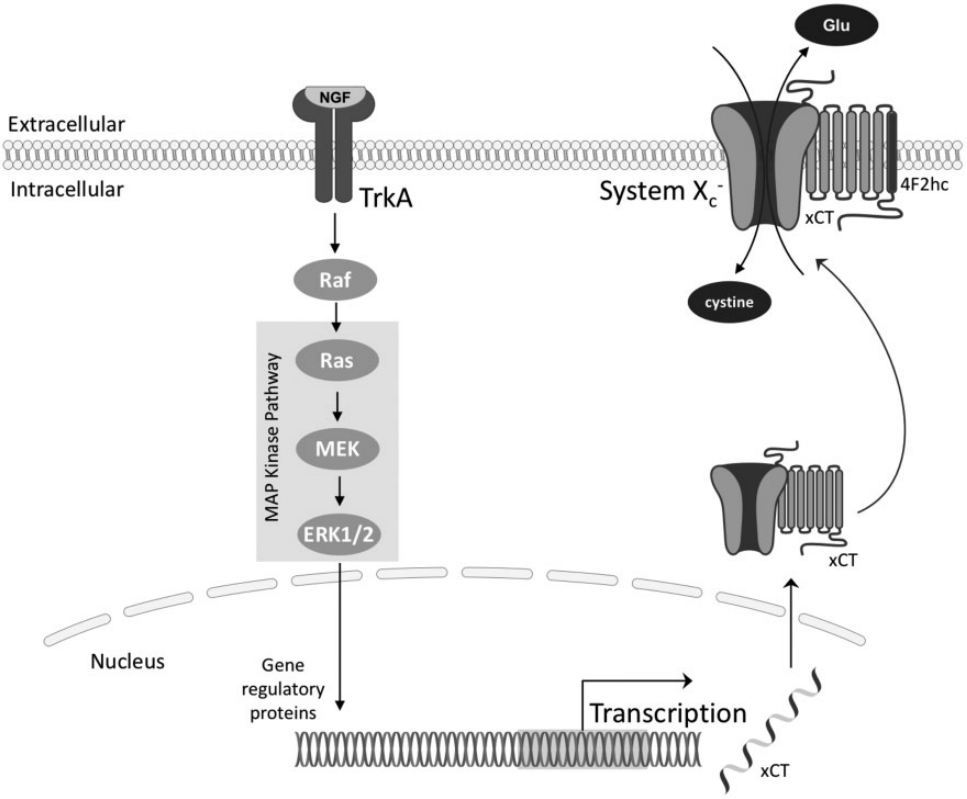

Figure 1. Proposed mechanism by which system x_C^--mediated glutamate release is regulated by TrkA-activated signalling pathways. NGF activates RAS-MAPK signalling through its tyrosine kinase receptor TrkA, which regulates xCT gene expression.

Materials and methods

In vitro

Cell culture. 4T1 triple-negative murine mammary gland carcinoma cells (American Type Culture Collection (ATCC)) were maintained in high glucose Roswell Park Memorial Institute (RPMI, Life Technologies); MDA-MB-231 triple-negative human breast carcinoma cells (ATCC) were maintained in high glucose Dulbecco's Modified Eagle's Medium (DMEM, Life Technologies). All cells were supplemented with 10% fetal bovine serum and 1% antibiotic/antimycotic (Life Technologies) incubated at 37°C and 5% CO_2 and verified to be mycoplasma free before experimental use.

Effect of TrkA inhibition on breast cancer cell number. The selective TrkA inhibitor tyrphostin AG879 (Sigma-Aldrich), a validated and specific inhibitor of TrkA,[34] was dissolved in dimethyl sulfoxide (DMSO) for preparation of a 79 mM stock. 4T1 and MDA-MB-231 cells were seeded at 5×10^3 cells/well in 96-well plates and treated with serial doses of AG879 from 50 μM through 3.125 μM dissolved in DMSO (maximum final concentration: 0.1%) or 0.1% DMSO alone (negative control).

Effect of NGF-TrkA on breast cancer cell number. Cell lines were seeded at 5×10^3 cells/well in 96-well plates and treated with various concentrations (0, 10 or 100 ng) of the recombinant human β-NGF protein (R&D Systems) in the presence of AG879 (6 μM) or control (DMSO) for 24 h, fixed with 10% neutral buffered formalin (NBF) and quantified using 0.1% Crystal Violet stain in 80% EtOH based on standard curves for each cell line. Absorbance was read on a spectrophotometer optical plate reader (BioTek) at $\lambda = 570$ nm.

Effects of NGF-TrkA on breast cancer cell metabolism. Cell lines were seeded and treated with serial doses of β-NGF (or phosphate-buffered saline (PBS)) in the presence or absence of AG879, as mentioned earlier, and incubated in 0.5 mg/mL 3-(4,5-Dimethylthiazol-2-yl)-2,5-diphenyltetrazolium bromide (MTT) labelling reagent (3-[4,5-dimethylthiazol-2-yl]-2,5-diphenyl tetrazolium bromide (Sigma-Aldrich) for the final 2 h of the 24-h treatment period. Absorbance was read on a spectrophotometer optical plate reader at $\lambda = 650$ nm.

Effects of NGF-TrkA on xCT protein level. Cells were treated with 100 ng β-NGF (or PBS) and 6 μM AG879 (or DMSO) for 24 h to determine the effects of NGF-TrkA activity on xCT protein levels, as quantified by Western blot analysis. Total protein concentrations were first determined using the Bio-Rad protein assay (Bio-Rad Laboratories) to ensure equal protein loading of whole cell lysates on 10% sodium dodecyl sulfate polyacrylamide gel electrophoresis gels and subsequent electrophoretic transfer to polyvinylidene difluoride membranes (Immobilon-P, Millipore Corporation). Expression of xCT was evaluated using respective primary antibody (Novus Biologicals), at a concentration of 1:1000, applied overnight at 4°C, with blocking in 5% skim milk in Tris-buffered saline with 0.1% Tween 20 (TBS-T). After washing, membranes were incubated in horseradish peroxidase-conjugated goat anti-rabbit secondary antibody (Santa Cruz) for 2 h at room temperature (RT) and visualized by enhanced chemiluminescence using an ECL-plus kit (GE Healthcare) on Amersham Hyperfilm (GE Healthcare). Calnexin (90 kDa) was used as a loading control. Processed blots were scanned and quantified using densitometry with ImageJ software (U.S. National Institutes of Health). Values were normalized to loading controls and compared to DMSO-treated control plates of the same cell line.

Effects of NGF-TrkA on xCT mRNA. mRNA was quantified using qualitative real-time polymerase chain reaction (qPCR) as previously described.[35] Briefly, 10^6 4T1 cells were seeded in 10 cm dishes and treated with 100 ng β-NGF in the presence (6 μM) or absence (DMSO) of the TrkA inhibitor AG879 for 24 h. Total RNA isolation from cell pellets was conducted using the Qiagen RNeasy kit (Qiagen Inc.). cDNA was then synthesized via reverse transcription using Superscript III and oligo DTs (Thermo Fisher Scientific), and qPCR assays were performed in duplicate using xCT primers (detailed in Table 1) and SsoAdvanced Universal SYBR Green Supermix (BioRad). Readings were normalized to the loading control Succinate Dehydrogenase Complex Flavoprotein Subunit A. Relative quantification analysis of gene expression data was conducted according to the $2^{-\Delta\Delta CT}$ method.

Effects of NGF-TrkA on ^{14}C-cystine uptake. The cellular uptake of radiolabelled ^{14}C-cystine was quantified, as cystine uptake is mediated by an exchange with glutamate via system x_C^-. The cystine uptake protocol was adapted from previous reports.[32,36] Briefly, 2×10^5 4T1 and MDA-MB-231 cells were seeded in 6-well plates and treated with 100 ng β-NGF, with or without 6 μM AG879 for 24 h. Media was then collected and stored at 4°C to quantify glutamate release (see below). Cultures were washed with Hank's Buffered Salt Solution (HBSS) and exposed to ^{14}C-cystine (0.015 mCi/mL) for 20 min at 37°C. Following ^{14}C-cystine exposure, cultures were washed with ice-cold HBSS to wash away excess extracellular cystine and dissolved in 220 μL of lysis buffer (0.1% Triton-X in 0.1 N NaOH) for 30 min. A 100 μL aliquot of each cell lysate was

Table 1. xCT primers used for relative qPCR.

Gene symbol	Primer sequences (5' to 3')	Reference gene	Product size (bp)	Melt peak (°C)
SLC7A11 (xCT)	FOR: CCTCTATTCGGACCCATTTAG REV: CTGGGTTTCTTGTCCCATATA	SDHA	99	80.0–80.5

Note: Melt peaks were obtained on a BioRad CFX Connect Real-TimeSystem. qPCR: qualitative real-time polymerase chain reaction; SDHA: Succinate Dehydrogenase Complex Flavoprotein Subunit A.

added to 1 mL Ecoscint-H scintillation fluid for quantification. Values were normalized to milligram of total protein using the Bradford protein assay (BioRad) and compared to ^{14}C-cystine uptake in DMSO-treated controls on the same experimental plate.

Effects of NGF-TrkA on glutamate release. Immediately prior to ^{14}C-cystine uptake quantification, growth media samples from 6-well plates were collected and stored at 4°C. Glutamate release was quantified using the AMPLEX Red glutamic acid assay kit (Invitrogen/Molecular Probes, Eugene, OR). This assay quantitates the fluorescent reaction product resorufin, which is produced in proportion to glutamate, for analysis on a CytoFluor Series, 4000 Fluorescence Multi-Well Plate Reader (PerSeptive Biosystems, Framingham, MA). To optimize this assay for measurement of media glutamate concentrations beyond 0.5 μM and eliminate the repeated cycling of glutamate and α-ketoglutarate, L-alanine and L-glutamate pyruvate transaminase were omitted from the reaction mixture. [37] Background glutamate from a media-only control well was subtracted from extracellular glutamate levels in culture media, and values were normalized to total protein using the Bradford protein assay, as mentioned earlier.

Immunocytochemistry. Immunocytochemistry was performed to confirm the presence of xCT on cultured 4T1 cells. Cells were seeded at 10^4 cells/well in 8-well chamber slides, fixed with 10% NBF, permeabilized with 0.1% Triton X-100, blocked with 1% bovine serum albumin, incubated in rabbit polyclonal anti-xCT primary antibody (Novus, 1:1000) for 1 h at RT and visualized using AlexaFluor-488 goat anti-rabbit secondary antibody (Life Technologies, 1:500) with 4',6-diamidino-2-phenylindole (DAPI) counterstain using EVOS FL Cell Imaging System.

In vivo

Mice. Experimentally naive immunocompetent female BALB/c mice (Charles River Laboratories) aged 4 to 6 weeks old upon arrival were group housed in cages maintained at 24°C with a 12-h light/dark cycle and provided ad libitum access to food and water. All animal procedures were performed according to guidelines established by the Canadian Council on Animal Care under a protocol reviewed and approved by the *Animal Research Ethics Board* of McMaster University.

Experimental groups. Mice (N = 26) were randomly assigned to three treatment groups: sham surgery +vehicle control (n = 9), tumour + vehicle control (n = 9) and tumour + AG879 (n = 8). Mice were inoculated with either 2×10^4 4T1 cells (n = 17) or an equal number of frozen/heat killed 4T1 cell sham controls (n = 9) injected percutaneously into the right distal femur to establish tumours. Drug treatment was delayed until 7 days post-4T1 cell inoculation to allow sufficient time for the implanted cells to reliably establish a bone tumour without drug interference, more accurately mimicking clinical conditions. Osmotic pump loading and implantation were performed in accordance with the manufacturer's specifications. AG879 was dissolved in DMSO and administered via intraperitoneally implanted Alzet model, 1002 mini-osmotic pumps (Durect) in a volume of 0.25 μL/h for a total of 5 mg/kg/day, based on the mean weight of the mice on the day of surgical implantation (20 g). Pumps were intraperitoneally implanted under isofluorane anaesthesia, and animals were systemically treated with AG879 from Day 7 post-cell inoculation through to end point.

All behavioural testing was performed with the groups being blinded, during the animals' light cycle. Animals were randomly assigned to systemic therapy or control groups and were acclimated to the behavioural testing environment and equipment one week prior to commencing data recording and were tested twice weekly for the duration of the experiment. The progression of spontaneous and evoked pain pre- and post-4T1 cell inoculation was monitored using a battery of tests for nociceptive behaviours: The dynamic weight bearing (DWB) system (BioSeb), the dynamic plantar aesthesiometer (DPA; Ugo Basile) and open-field observations, including spontaneous guarding time and limb use. Three behavioural tests were performed prior to experiment Day 0 which served to establish a stable baseline for the animals' normal behaviour; results are expressed for each animal as a percentage of these baseline scores. Behavioural testing occurred on days 6, 9, 13, 16 and 20 post-inoculation, and animals that had not yet reached end point were sacrificed on Day 21.

Spontaneous pain. Open-field tests, including spontaneous guarding of the affected limb and limb use, were used to visually assess ongoing and ambulatory nociception using previously validated tests.[38] The time (s) spent spontaneously guarding the hindpaw represented ongoing pain and was recorded during a 5-min open-field observation period using a stopwatch. Guarding time was defined as the time the hindpaw was held aloft while ambulatory. During the 5-min spontaneous ambulation period, normal hindlimb use was observed and scored on a scale of 4 to 0: (4) normal use, (3) slight limp, (2) limp and guarding behaviour, (1) partial non-use of the limb in locomotor activity and (0) complete lack of limb use.

The DWB quantitates spontaneous pain-related discomfort and postural disequilibrium[39] by recording the weight distribution of each point of contact of freely moving animals via a sensor pad covering the entire floor surface of the testing chamber. Weight-bearing data were directly captured at a sampling rate of 10 Hz, and the animals' position on the sensor was manually validated following data collection using respective software (DWB v.1.3.4.36). To reduce experimenter bias and ensure spatial and temporal objectivity, a video camera recorded the animals' position within the testing chamber over the capture period. Postural disequilibrium was defined as favouring the tumour-bearing limb and a compensatory shift of weight bearing to other body parts and was considered indirect evidence of nociception. Data for each test day were calculated as a mean weight recorded for all points of weight bearing and expressed as a single measurement of the weight borne by the affected limb as a ratio of the total weight recorded at each frame within the capture period. Data were normalized to the baseline scores prior to cancer cell inoculation for each mouse. A relative reduction in weight borne by the ipsilateral paw was considered evidence of postural disequilibrium.

Evoked pain. The DPA test, which is a semi-automated version of the classic von Frey test,[40] was used to quantify mechanical allodynia and hyperalgesia in mice pre- and post-tumour cell inoculation. A mechanical metal filament was raised by an electrical actuator with variable force and acceleration. The filament stimulated the plantar surface of the affected hindpaw and contralateral hindlimb, and the threshold force and time at which each animal withdrew its paw were recorded. The average force of four independent measurements collected from each paw on each test day was calculated, and mean values were normalized to individual animal's baseline DPA values. A reduction in force required to elicit paw withdrawal in the tumour-bearing limb was considered indicative of hypersensitivity manifested as deliberate withdrawal of the affected paw from the filament pressure.

Tumour xenografts. The 4T1 mammary carcinoma cell line is highly tumourigenic and invasive; the growth and metastatic spread of these cells in BALB/c mice very closely mimic human breast cancer in its proliferative and metastatic characteristics.[41] Thus, this tumour was used as an animal model for stage IV human breast cancer. On experimental Day 0, mice were anaesthetized by isoflurane inhalation and injected with buprenorphine (0.05 mg/kg, subcutaneous; Schering-Plough) to mitigate surgically induced discomfort. Animals were inoculated with 2×10^4 4T1 cells suspended in 25 μL sterile PBS percutaneously into the right distal femur. Mice were laid supine with the ipsilateral stifle joint bent to 90° to clear the patella and minimize tissue damage. A 26-gauge needle was then manually inserted between the medial and lateral condyles of the distal epiphysis by delicate rotation parallel to the longitudinal axis of the femur to breach the cortical bone. Once within the bone epiphysis, the injectate was slowly infused over the course of approximately 1 min. The contralateral hindlimb served as a negative control specific to each animal. This method of intrafemoral injection was selected to minimize damage to the surrounding tissues and has been successfully applied in mouse[6] and rat[42] models of bone cancer-induced nociceptive behaviour.

Transcardial perfusion and tissue collection. Throughout tumour development, each animal was monitored daily for limb use, overall health status and body weight. Animals were euthanized by transcardial perfusion when they no longer bore weight on the affected hindlimb. This experimental end point occurred on or before Day 21 post-tumour cell inoculation for all animals. Under sodium pentobarbital anesthetic (90 mg/kg, ip.), animals were perfused with 100 mL cold PBS, immediately followed by 100 mL cold 4% paraformaldehyde (PFA). Tumour-bearing femurs and surrounding tissues were dissected, X-rayed, post-fixed in 4% PFA for 48 h, decalcified in 10% Ethylenediaminetetraacetic acid (EDTA) for 14 days and paraffin-embedded for histological analyses.

Ex vivo

Radiographic analysis. High-resolution radiographic analysis was used to establish the extent of bone degradation in ipsilateral hindlimbs immediately following perfusion, with substantial bone degradation considered to be evidence of tumour invasion. X-ray scans of all mice were collected using a Faxitron MX-20 X-ray system (Faxitron X-ray Co., Wheeling, IL) on Kodak MIN-R, 2000 Mammography film (Eastman Kodak, Rochester,

NY). Affected hindlimbs were scored on a scale of 0 to 3: (0) normal bone, no visible lesion; (1) minor loss of bone density, minimal lesion; (2) Moderate to substantial loss of bone density, lesion limited to bone trabecula and cortex and (3) substantial loss of bone density, lesion includes clear periosteal involvement or fracture.

Hematoxylin and eosin. Ipsilateral hindlimbs were stained with hematoxylin and eosin to confirm the degree of intrafemoral tumour in animals that demonstrated lytic lesions on X-rays. Following decalcification, femurs and surrounding tissues were paraffin-embedded, sagittally sectioned at 5 μm, slide mounted, stained and xylene-cleared for microscopy.

Immunofluorescence. Immediately adjacent serial hindlimb sections from the same paraffin block were processed for immunofluorescence; following antigen retrieval in EDTA (pH 8, 95°C) for 30 min, sections were incubated in respective primary antibodies (xCT: Novus, 1:1000; cytokeratin 7: Santa Cruz, 1:500) overnight at 4°C, washed in PBS, incubated in 1:500 fluorescent secondary antibodies (Life Technologies AlexaFluor-488 goat anti-rabbit and AlexaFluor-647 goat anti-mouse, respectively) for 2 h at RT, counterstained with DAPI and coverslipped.

Statistical analyses

In vitro. For each cell line, a one-way analysis of variance (ANOVA) with Bonferroni post hoc comparisons was used to assess the dose response of AG879 on cell number. A two-way ANOVA with Bonferroni post hoc comparisons was then used to assess the effect of serial dilutions of β-NGF for each cell line, in the presence and absence of 6 μM AG879, on cell number and metabolism. Separate two-way ANOVAs with Bonferroni post hoc comparisons were used to assess the effect of β-NGF and AG879 on xCT protein levels and mRNA levels for each cell line. One-way ANOVAs with Bonferroni post hoc comparisons were used to assess the dose effect of β-NGF on functional system x_C^- activity, as measured by cystine uptake and glutamate release. Independent *t* tests were then used to assess the effect of AG879 on cystine uptake relative to cells treated with each β-NGF dose.

In vivo. DWB and DPA data sets were analyzed to derive survival curves comparing the time until respective behavioural scores fell irreversibly below 50% of the animals' baseline nociceptive responses. For Kaplan–Meier curve analyses of 50% threshold pain data (time to behavioural decline) in DWB and DPA behavioural tests, chi-square analyses were used.

Ex vivo. Chi-square analysis of the proportion of scores within each treatment group was used to assess radiographic analysis of osteolysis. Immunocytochemical staining of xCT in 4T1 cells and immunofluorescent staining of xCT within ipsilateral hindlimbs were qualitatively considered.

All analyses were performed using GraphPad Prism 5.0a software (GraphPad Software, Inc., La Jolla, CA) and GraphPad QuickCals; α was set at 0.05. Data are expressed as means ± standard error of the mean from three independent experiments, unless otherwise stated.

Results

In vitro

AG879 influences breast cancer cell number. Selective TrkA inhibition appeared to concentration-dependently decrease cell number in 4T1 and MDA-MB-231 triple-negative cells, such that higher doses of AG879 (i.e., 12.5, 25 and 50 μM AG879) decreased cell number relative to DMSO-treated controls after 24 h treatment (see Table 2). Treatment with 6 μM AG879 did not significantly alter 4T1 or MDA-MB-231 cell growth or metabolism as measured by Crystal Violet and MTT assays. Thus, this dose was selected for all further in vitro studies.

Selected AG879 and NGF doses do not affect 4T1 cell metabolism. Treatment with β-NGF (0.01–100 ng) or AG879 (6 μM) for 24 h did not significantly affect breast cancer cell number (data not shown) or metabolism (Figure 2).

Table 2. Values compared to DMSO control

	3 μM	6 μM	12 μM	25 μM	50 μM
4T1	1.08 ± 0.04	0.87 ± 0.07	0.8 ± 0.04*	0.66 ± 0.07**	0.35 ± 0.02**
MDA-MB-231	0.75 ± 0.06*	0.85 ± 0.06	0.65 ± 0.11*	0.55 ± 0.05*	0.39 ± 0.05*

Note: Murine 4T1 and human MDA-MB-231 carcinoma cells were seeded and treated with serial doses of AG879 for 24 h, and cell number was quantified using crystal violet staining. Values indicate mean ± SEM fold change in cell number compared to DMSO negative control (0 μM AG879), data are from three independent experiments.
Values compared to DMSO control, *$p < 0.05$, **$p < 0.005$.

AG879 attenuates β-NGF-induced increases in xCT protein in 4T1 cells. Western blotting analysis confirmed the presence of TrkA on 4T1 and MDA-MB-231 cells (data not shown). Blots also demonstrated a marked increase in xCT bands at 37 kDa in cells treated with 100 ng β-NGF in both 4T1 and MDA-MB-231 cell lines, an effect which was attenuated by AG879 in 4T1 murine carcinoma cells, with a similar, albeit modest, trend observed in MDA-MB-231 cells (Figure 3).

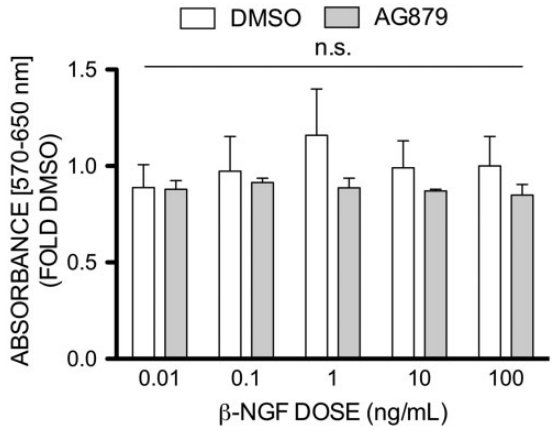

Figure 2. Treatment with β-NGF or AG879 does not significantly affect 4T1 carcinoma cell metabolism. 4T1 murine carcinoma cells were seeded and treated with 0.01 to 100 ng β-NGF in the presence or absence of 6 μM AG879 and the MTT assay was utilized during the last 2 h of the 24-h drug treatment period to quantitate cellular metabolic activity. Bars indicate mean ± SEM fold change compared to DMSO negative control. Data are from three independent experiments, $\alpha = 0.05$. DMSO: dimethyl sulfoxide; NGF: nerve growth factor.

AG879 attenuates β-NGF-induced increases in xCT mRNA in 4T1 cells. qPCR analysis demonstrated a marked increase in xCT mRNA in 4T1 cells treated with 100 ng β-NGF, an effect which was attenuated by treatment with 6 μM AG879 (Figure 4).

AG879 decreases functional system x_C^- activity. In 4T1 cells, ^{14}C-cystine uptake was markedly reduced in cells treated with 6 μM AG879 for 24 h relative to DMSO- and 10 ng β-NGF-treated cells. Treatment with β-NGF appeared to marginally increase ^{14}C-cystine uptake relative to DMSO control; however, this effect was not statistically significant (Figure 5(a) and (b)). Accordingly, glutamate release was increased in cells treated with 10 ng and 100 ng β-NGF (Figure 5(c)). Furthermore, treatment with 6 μM AG879 appeared to decrease this effect, although this trend was not statistically significant (Figure 5(c)). A similar trend was observed in triple-negative human MDA-MB-231 cells (data not shown).

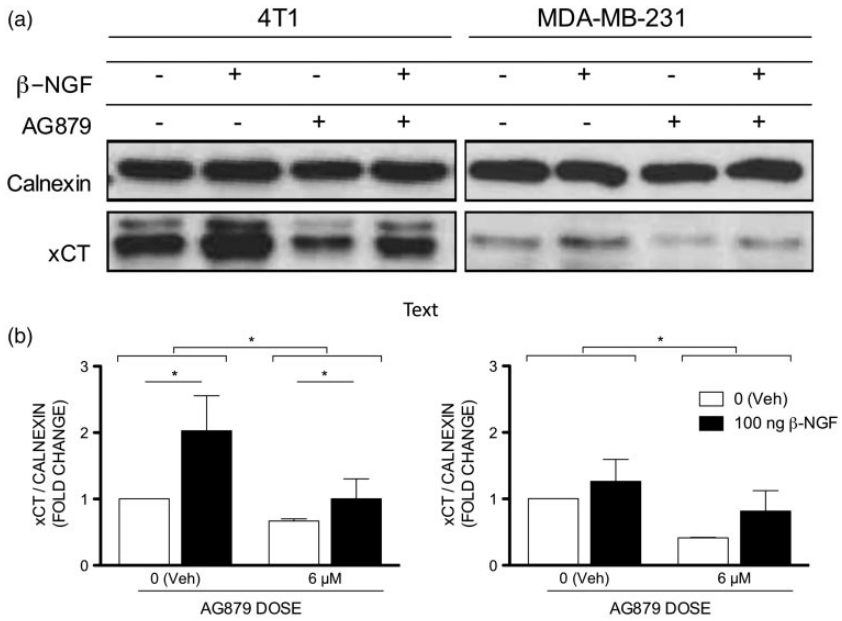

Figure 3. AG879 attenuates β-NGF-induced increase in xCT protein in carcinoma cells. xCT is expressed by murine 4T1 and human MDA-MB-231 breast cancer cells. Treatment with AG879 (6 μM, 24 h) reduces xCT protein levels in 4T1 and MDA-MB-231 cells relative to vehicle-treated cells and significantly attenuates β-NGF-induced increase in xCT protein levels in murine 4T1 cells. (a) Representative xCT protein levels in cells treated with 6 μM AG879 (or DMSO) and 100 ng β-NGF (or PBS) for 24 h. (b) Relative expression of xCT (37 kDa) compared to DMSO-treated control plates of the same cell line, as determined by densitometry analysis. Data are from three independent experiments, normalized to Calnexin (90 kDa) and are expressed as means ± SEM, $\alpha = 0.05$. NGF: nerve growth factor.

In vivo

AG879 attenuates tumour-induced nociceptive behaviours. The TrkA inhibitor AG879 appeared to delay the onset of nociception, as measured by progressively impaired limb use and increased spontaneous guarding scores (Figure 6 (a) and (b), respectively). In both the DWB (Figure 7(a)) and the DPA (Figure 7(b)), tumour-bearing mice exhibited significantly greater pain behaviours compared to their sham controls from Day 9 post-tumour cell inoculation until end point. AG879 significantly delayed behavioural decline, as measured by postural disequilibrium in the DWB, indicating that significantly fewer tumour-bearing animals fell below 50% of their individual baseline nociceptive score when treated with AG879 (Figure 7(a)). In the DPA, a similar trend was observed, with fewer AG879-treated animals falling below 50% of their individual baseline scores, but this effect was not statistically significant (Figure 7(b)).

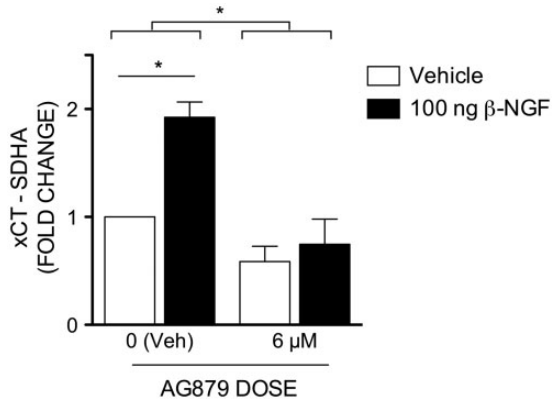

Figure 4. AG879 attenuates β-NGF-induced increase in xCT mRNA in carcinoma cells. xCT mRNA in murine 4T1 carcinoma cells treated with DMSO and β-NGF, relative to negative control. Data are from three independent experiments, normalized to SDHA and are expressed as means ± SEM, $\alpha = 0.05$. NGF: nerve growth factor; SDHA: Succinate Dehydrogenase Complex Flavoprotein Subunit A.

Ex vivo

AG879 impedes tumour invasion in vivo. Radiographic analysis confirmed the presence of bone degradation in cancer cell-inoculated mice at end point and AG879 appeared to partially attenuate tumour-induced osteolysis (Figure 8(a)). Hematoxylin and eosin staining of ipsilateral hindlimbs confirmed the presence of tumour cells in femurs of animals that demonstrated lytic lesions in radiographic X-rays; tumour invasion was most frequently observed in the distal epiphysis and diaphysis of ipsilateral femurs. AG879-treated mice demonstrated marginally less osteolytic activity, with generally smaller tumours observed in drug-treated animals (see Figure 8(b) and (c) for representative images), in accordance with radiographic lesion scores.

AG879 inhibits xCT expression in vivo. Immunocytochemistry confirmed the presence of xCT on 4T1 murine carcinoma cells in vitro (Figure 9(a)), and immunofluorescent staining of ipsilateral femurs demonstrated the presence of the epithelial marker cytokeratin 7 (Figure 9(b)), confirming the presence of breast cancer cells within the bone environment at end point. Double-label immunofluorescence demonstrated the

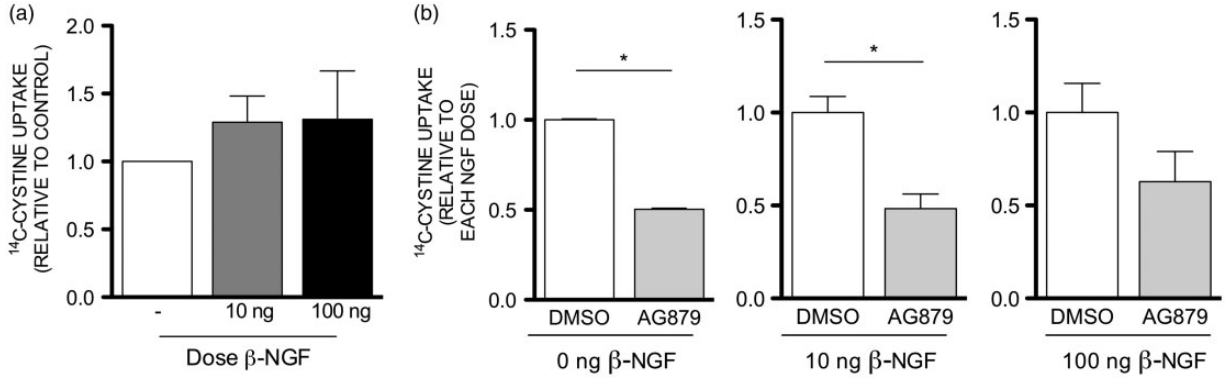

Figure 5. Functional system x_C^- activity is increased by β-NGF and attenuated by TrkA inhibition in murine 4T1 carcinoma cells. Treatment with β-NGF for 24 h demonstrated a dose-dependent trend of increased ^{14}C-cystine uptake in 4T1 cells relative to DMSO control, although this effect was not statistically significant (a). 4T1 cells treated with 6 μM AG879 for 24 h demonstrated a relative decrease in ^{14}C-cystine uptake relative to corresponding doses of β-NGF (b). Accordingly, a similar trend was observed in media levels of glutamate: treatment with β-NGF dose-dependently increased glutamate release, such that treatment with 10 ng and 100 ng β-NGF significantly increased media glutamate by 1.8- and 2-fold, respectively, relative to DMSO control (c). 4T1 cells treated with 6 μM AG879 demonstrated decreased glutamate release when matched to NGF doses, although the trend was not statistically significant (d). Data are from three independent experiments, normalized to protein level and are expressed as means ± SEM relative to DMSO, *significantly different from DMSO control, $\alpha = 0.05$. DMSO: dimethyl sulfoxide; NGF: nerve growth factor.

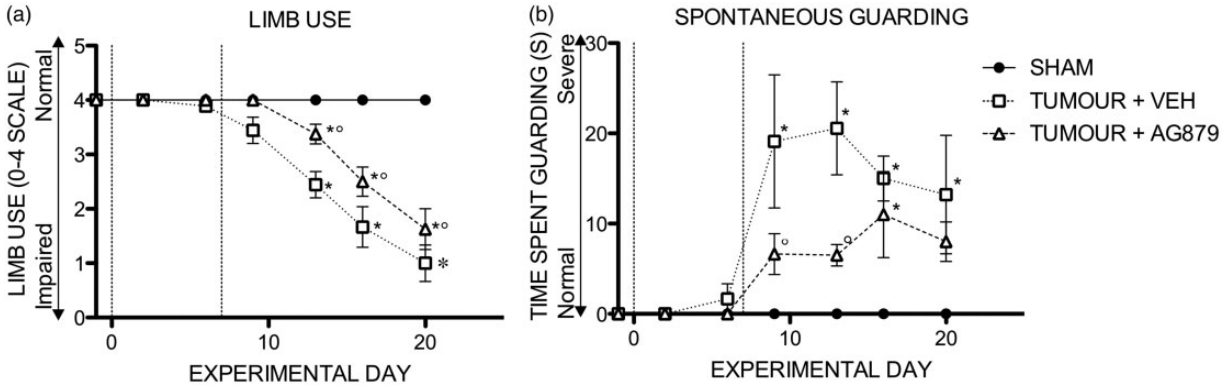

Figure 6. AG879 significantly delays the onset and severity of spontaneous nociceptive behaviours. Open-field tests, including time spent spontaneously guarding the affected limb and scaled limb use, were used to visually assess ongoing and ambulatory nociception. (a) Quantification of limb use in the ipsilateral femurs throughout tumour progression. Normal hindlimb use during spontaneous ambulation was observed and scored on a scale of 4 to 0: Points indicate mean ± SEM of each stage of bone destruction as quantified by this scale. Limb use numbers represent: (4) normal use, (3) pronounced limp, (2) limp and guarding behaviour, (1) partial non-use of the limb in locomotor activity and (0) complete lack of limb use. (b) Time spent spontaneously guarding the hindpaw represented ongoing pain and was recorded during an open-field observation period. Guarding time was defined as the time (s) the hindpaw was held aloft while ambulatory. Points indicate means ± SEM; *significantly different from SHAM, significantly different from TUMOUR, $\alpha = 0.05$; Vertical dashed lines indicate intrafemoral injections (Day 0) and start of treatment (Day 7).

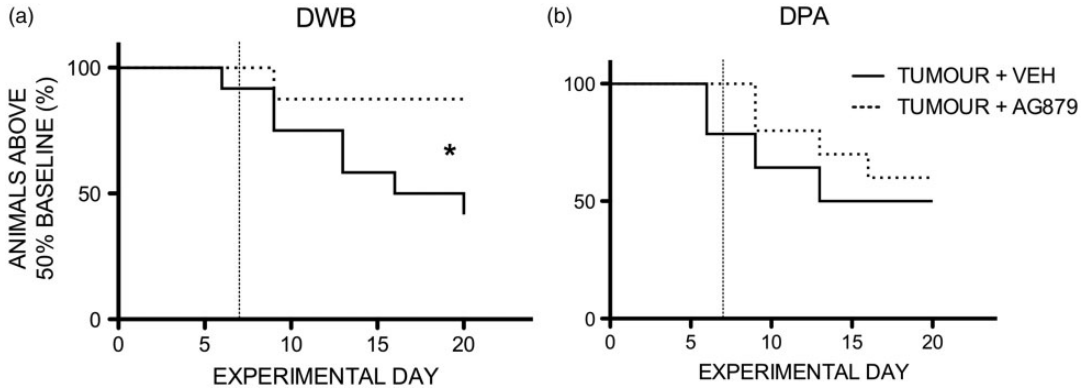

Figure 7. AG879 delays time until behavioural decline. (a) The DWB quantitates the weight borne by the affected limb as a percentage of total recorded weight, standardized to baseline scores. Thus, 100% on the *y*-axis represents behaviour prior to tumour inoculation; less than 100% indicates a decrease in weight borne by the tumour-afflicted limb and is indicative of nociceptive behaviour. Kaplan–Meier curve analysis of the time until behavioural decline, expressed as a percentage of animals above the 50% of baseline cutoff, shows AG879 significantly delays time until the onset of postural disequilibrium in the DWB (chi square = 0.018, p = 0.724). (b) The DPA test quantitates the threshold force at which the animal withdraws from a progressive stimulus applied to the plantar surface of the affected hindpaw. Thus, 100% on the *y*-axis is equivalent to baseline behaviour prior to tumour inoculation; less than 100% indicates a decrease in the force withstood by the tumour-bearing limb. Kaplan–Meier curve analysis of the time until behavioural decline shows AG879 marginally, but not significantly, reduced time until decline in the DPA (chi square = 4.465, p = 0.1). Vertical dashed lines indicate start of treatment (Day 7). DWB: dynamic weight bearing; DPA: dynamic plantar aesthesiometer.

overlapping distribution of xCT with breast cancer cells in ipsilateral femurs (Figure 9(c)), confirming the expression of xCT on 4T1 cells in vivo. AG879 appeared to markedly inhibit xCT expression by tumour cells (Figure 9(d)).

Discussion

Cancer pain is highly heterogeneous and is thought to be the result of varied pathological mechanisms. Current treatment options often induce severe dose-dependent side effects and fail to adequately manage advanced breast CIBP. Clinically, achieving analgesia often comes at the expense of patients' quality of life. The complexity of CIBP is partly due to the unique properties of the affected tissue; osteoclastogenesis,[43] inflammation,[44,45] increased neurotrophic activity,[20,23] demyelination,[46] and extracellular acidification[45] created by the presence of bone tumours have been implicated in the sensitization of surrounding nociceptors and may

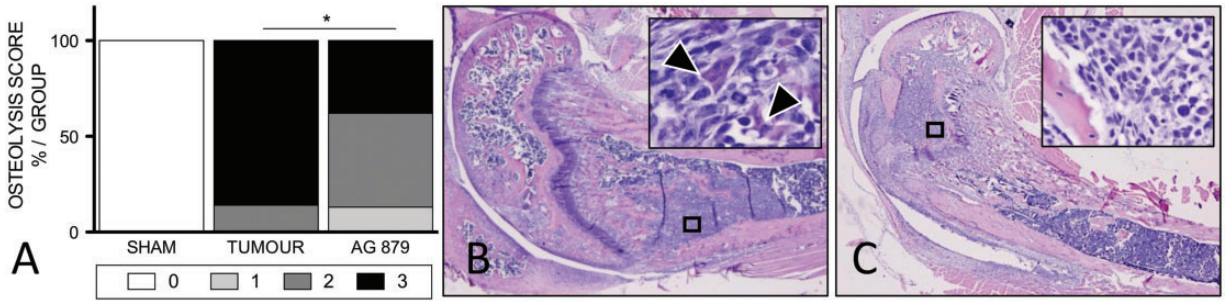

Figure 8. AG879 attenuates tumour-induced femoral osteolysis. (a) Quantification of bone osteolysis in the ipsilateral femurs at end point of all treatment groups on 0 to 3 radiographic analysis scale. Numbers represent: (0) normal bone, no visible lesion; (1) minor loss of bone density, marginal lesion; (2) considerable loss of bone density, lesion limited to bone trabeculae and cortex; (3) substantial loss of bone density, lesion suggests periosteal involvement and/or fracture. Osteolytic scores are expressed as total percentage per treatment group in each score category at end point, *significantly different from sham, $\alpha = 0.05$. Representative hematoxylin and eosin staining of ipsilateral femurs in vehicle (d) and PLX3397-treated (f) tumour-inoculated mice at end point, 10× magnification. Boxed areas indicate areas of tumour invasion, inserts depict enlarged tumour cell boxes at 60× magnification, arrow heads indicate osteoclasts.

cumulatively contribute to cancer-induced hyperalgesia. Among other influences, it is clear that glutamate dysregulation[47] and aberrant neurotrophic activity[27,48] may contribute to CIBP through pathological osteoclastogenesis and sensitization. The production and vesicular secretion of NGF drives the autocrine stimulation and proliferation of breast cancer cells through its cognate receptor, TrkA.[10] In the present study, we have demonstrated that inhibiting the NGF-TrkA complex may limit CIBP, conceivably through downstream effects on system x_C^-. Extensive research supports the hypothesis that NGF drives cancer pain through pathological nerve sprouting[20,24,27,28]; this study provides evidence that the effects of NGF on breast cancer cells and surrounding cells in the tumour microenvironment may not be limited to its conventionally accepted neurotrophic actions. The discovery that NGF and system x_C^- may be functionally interconnected provides a novel approach to indirectly targeting system x_C^- for CIBP relief.

In vitro, AG879 dose-dependently reduced breast cancer cell growth, in accord with previous findings.[49] More importantly, however, a dose which did not effectively alter cell number or metabolism significantly inhibited the functional activity of system x_C^-. That is, AG879 markedly reduced cystine uptake in 4T1 carcinoma cells in the presence and absence of β-NGF. One possible explanation for the relationship between NGF and system x_C^- is through changes that occur at the level of xCT by activation of the mitogen-activated protein kinase (MAPK)/extracellular signal-regulated kinase (ERK) signalling pathway. Through TrkA, NGF is known to activate Ras-MAPK signalling (reviewed in Huang and Reichardt[50]). Interestingly, serine kinases, including MAPK, phosphorylate signal transducer and activator of transcription 3 (STAT3), which then homo- or heterodimerizes and translocates into the nucleus.[35,51,52] where it then binds specific DNA recognition elements to regulate expression of genes, including xCT.[51] In MDA-MB-231 breast cancer cells, for example, the MAPK inhibitor PD098059 abolishes basal xCT transcriptional activity.[51] Furthermore, STAT3 activation is coupled with increased system x_C^- activity. Accordingly, sustained treatment with the STAT3 inhibitor SH-4-54 decreases xCT expression and system x_C^- activity in MDA-MB-231 cells.[51] It is therefore plausible that phosphorylated TrkA contributes to xCT expression through MAPK and/or STAT3 signalling, although further research is required to explore the specific pathways involved in this relationship.

A consistent trend was observed across both cell lines assayed in vitro; AG879 influenced functional system x_C^- activity in murine 4T1 and human MDA-MB-231 carcinoma cells. Thus, to mitigate the number of animals employed and avoid the complexity of using human cancer cells in an immunocompromised animal model, a syngeneic mouse model was utilized to characterize the effects of TrkA on cancer progression and CIBP in vivo. The battery of tests for nociceptive behaviours was cumulatively selected to reflect what is observed in patients who protect or suspend their afflicted limb.

Inhibition of TrkA delayed the onset of nociceptive behaviours in tumour-bearing mice, as demonstrated by spontaneous guarding and limb use scores, as well as time until behavioural decline in the DWB. No significant reduction in evoked pain was observed in the DPA, suggesting that either NGF-TrkA signalling or functional system x_C^- activity may be more implicated in spontaneous than evoked pain. Previous work has shown that early but not late administration of an NGF sequestering antibody can prevent the onset of tumour-induced nerve sprouting in a mouse model of CIBP.[20] Here, pharmacological TrkA inhibition began on Day 7 after intrafemoral cancer cell inoculation, corresponding with initial behavioural indications of CIBP. This time point

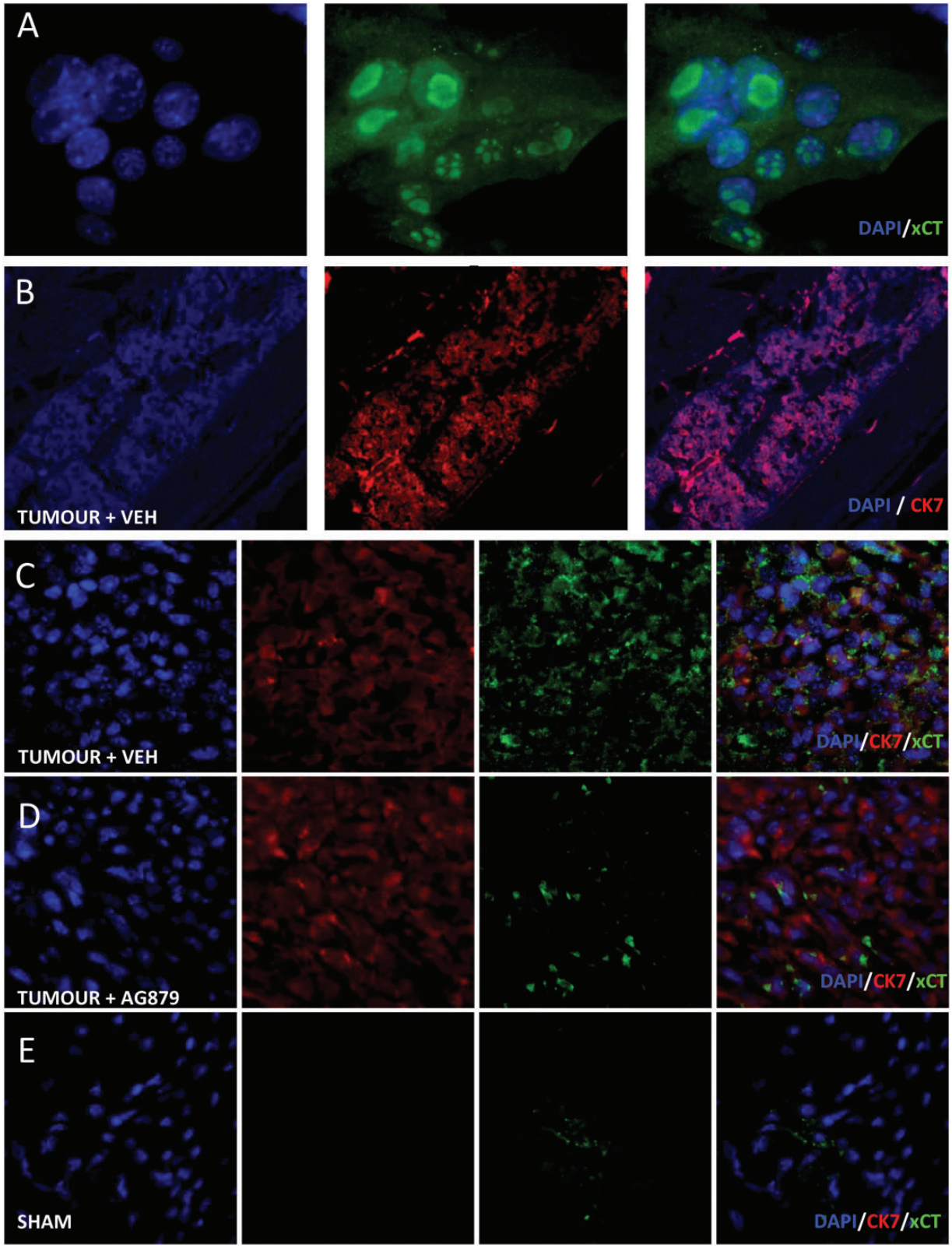

Figure 9. AG879 inhibits xCT expression in 4T1 murine carcinoma cells. Immunocytochemical staining of xCT in murine 4T1 mammary carcinoma cells in vitro at 60× magnification (a). Immediately adjacent serial sections to hematoxylin and eosin-stained femurs were stained for nuclei (blue), cytokeratin 7 (CK7) and xCT (green) and imaged using EVOS FL Cell Imaging System at 10× dry (b) and 60× oil (c–e) immersion lenses: double-label immunofluorescent staining of epithelial marker CK7 and xCT in representative tumour-inoculated animals (b), vehicle- (c) and AG879-treated (d) tumour-bearing femurs and sham control (e).

represents a relative late administration regimen to mimic what is seen clinically, as patients are often not diagnosed until metastases have progressed to an advanced, often painful, state. The ability of AG879 to partially mitigate, but not abolish, nociceptive behaviours when administered relatively late, with the onset of pain, suggests that irreversible damage to the bone microenvironment may have already occurred, but that this inhibitor nevertheless had subsequent effects on additional targets implicated in nociception.

The cystine-coupled export of glutamate through system x_C^- bears additional significance within the nervous system, as it represents a non-vesicular route by which this excitatory neurotransmitter can activate glutamate receptors on sympathetic nerve fibres, particularly those present in extrasynaptic locales. While glutamate is recognized as a ubiquitous cell signalling molecule and critical intercellular neurotransmitter, excessive glutamate efflux produces an excitotoxic environment. One means by which glutamate may directly contribute to nociception is by acting on adjacent afferent nociceptive neurons within the bone. Another means by which glutamate evokes nociception is by influencing many aspects of metabolic homeostasis during normal bone remodelling,[47,53,54] affecting the communication between osteoblasts and osteoclasts, which maintain a delicate balance of bone formation and resorption, respectively.[37,54] The disruption of glutamatergic signalling within the bone microenvironment influences cell differentiation[55,56] and function.[47,57,58] In the presence of bone metastases, the balance between bone formation and degradation is disturbed.[59] Disruption of this homeostasis by the aberrant increase in glutamate released from breast cancer cells into the bone microenvironment leads to excessive osteoclastogenesis[60–62] and reduced bone mineralization.[63] Given that glutamate released by system x_C^- can directly stimulate adjacent afferent nociceptors, disrupt normal bone remodelling and inhibit bone mineralization, the observed delay until the time of onset of nociception is a logical consequence of inhibiting system x_C^-. Accordingly, the reduced osteolysis seen in AG879-treated animals, relative to untreated tumour-bearing animals, is reflective of the observed delay in nociceptive behaviours and reduction in functional system x_C^- activity seen in the in vivo and in vitro data, respectively and cumulatively suggests that TrkA may be implicated in the osteolytic contribution to cancer pain.

Our group has reported on the antinociceptive effects of the steric system x_C^- inhibitor, sulfasalazine (SSZ) in a validated model of CIBP in which SSZ delayed the onset of tumour-induced nociception,[6] an outcome which has since been validated in a syngeneic mouse model.[7] However, despite its efficacy in animal models of CIBP, SSZ has limited translational capacity given the poor bioavailability of the parent drug relative to its metabolites. Furthermore, side effects of SSZ mirror many of the symptoms already observed in cancer patients, including nausea, vomiting and anorexia, symptoms which ought to be controlled, not exacerbated. Therefore, although system x_C^- is a promising pharmacological target for the treatment of CIBP, novel inhibitors are needed to better manage this pain without the negative side effects that accompany SSZ.

The present study corroborates the role of aberrant glutamate secretion through system x_C^- in breast CIBP and suggests the possibility of a feedback loop between NGF and system x_C^-. The role of glutamate in cancer cell metabolism and the effects of NGF on system x_C^--mediated glutamate output suggest that this connection may be vital to the progression of cancer pain. The relationship between TrkA and system x_C^- is an important link in elucidating breast cancer-induced pain signalling. The present study supports the pharmacological inhibition of glutamate release to limit nociception and connects increases in glutamate release to previously unrelated increases in NGF. This study suggests that the actions of NGF extend beyond its conventionally recognized roles of neuronal survival and differentiation. Indirectly inhibiting system x_C^- through the pharmacological modulation of TrkA therefore presents a valuable target for therapeutic intervention in the treatment of cancer pain.

Acknowledgements

The authors wish to thank Dr Mark Inman for his expert advice in statistical analyses.

Declaration of Conflicting Interests

The author(s) declared no potential conflicts of interest with respect to the research, authorship, and/or publication of this article.

Funding

The author(s) disclosed receipt of the following financial support for the research, authorship, and/or publication of this article: This work was supported by the Canadian Breast Cancer Foundation to GS.

ORCID iD

Tanya Miladinovic http://orcid.org/0000-0002-4129-7950

References

1. Seidlitz EP, Sharma MK, Saikali Z, Ghert M and Singh G. Cancer cell lines release glutamate into the extracellular environment. *Clin Exp Metastasis* 2009; 26: 781–787.
2. Sharma MK, Seidlitz EP and Singh G. Cancer cells release glutamate via the cystine/glutamate antiporter. *Biochem Biophys Res Commun* 2010; 391: 91–95.

3. Choi DW. Glutamate receptors and the induction of excitotoxic neuronal death. *Prog Brain Res* 1994; 100: 47–51.
4. Choi DW, Maulucci-Gedde M and Kriegstein AR. Glutamate neurotoxicity in cortical cell culture. *J Neurosci* 1987; 7: 357–368.
5. Miladinovic T, Nashed MG and Singh G. Overview of glutamatergic dysregulation in central pathologies. *Biomolecules* 2015; 5: 3112–3141.
6. Ungard RG, Seidlitz EP and Singh G. Inhibition of breast cancer-cell glutamate release with sulfasalazine limits cancer-induced bone pain. *Pain* 2014; 155: 28–36.
7. Slosky LM, BassiriRad NM, Symons AM, Thompson M, Doyle T, Forte BL, Staatz WD, Bui L, Neumann WL, Mantyh PW, Salvemini D, Largent-Milnes TM and Vanderah TW. The cystine/glutamate antiporter system xc^- drives breast tumour cell glutamate release and cancer-induced bone pain. *Pain* 2016; 157: 2605–2616.
8. Descamps S, Toillon RA, Adriaenssens E, Pawlowski V, Cool SM, Nurcombe V, Le Bourhis X, Boilly B, Peyrat JP and Hondermarck H. Nerve growth factor stimulates proliferation and survival of human breast cancer cells through two distinct signaling pathways. *J Biol Chem* 2001; 276: 17864–17870.
9. Descamps S, Lebourhis X, Delehedde M, Boilly B and Hondermarck H. Nerve growth factor is mitogenic for cancerous but not normal human breast epithelial cells. *J Biol Chem* 1998; 273: 16659–16662.
10. Dollé L, El Yazidi-Belkoura I, Adriaenssens E, Nurcombe V and Hondermarck H. Nerve growth factor overexpression and autocrine loop in breast cancer cells. *Oncogene* 2003; 22: 5592–5601.
11. Lowe EM, Anand P, Terenghi G, Williams-Chestnut RE, Sinicropi DV and Osborne JL. Increased nerve growth factor levels in the urinary bladder of women with idiopathic sensory urgency and interstitial cystitis. *Br J Urol* 1997; 79: 572–577.
12. Aloe L, Tuveri MA, Carcassi U and Levi-Montalcini R. Nerve growth factor in the synovial fluid of patients with chronic arthritis. *Arthritis Rheum* 1992; 35: 351–355.
13. Halliday DA, Zettler C, Rush RA, Scicchitano R and McNeil JD. Elevated nerve growth factor levels in the synovial fluid of patients with inflammatory joint disease. *Neurochem Res* 1998; 23: 919–922.
14. Friess H, Zhu ZW, di Mola FF, Kulli C, Graber HU, Andren-Sandberg A, Zimmermann A, Korc M, Reinshagen M and Büchler MW. Nerve growth factor and its high-affinity receptor in chronic pancreatitis. *Ann Surg* 1999; 230: 615–624.
15. Wang W, Chen J and Guo X. The role of nerve growth factor and its receptors in tumorigenesis and cancer pain. *Biosci Trends* 2014; 8: 68–74.
16. Crowley C, Spencer SD, Nishimura MC, Chen KS, Pitts-Meek S, Armanini MP, Ling LH, McMahon SB, Shelton DL and Levinson AD. Mice lacking nerve growth factor display perinatal loss of sensory and sympathetic neurons yet develop basal forebrain cholinergic neurons. *Cell* 1994; 76: 1001–1011.
17. Smeyne RJ, Klein R, Schnapp A, Long LK, Bryant S, Lewin A, Lira SA and Barbacid M. Severe sensory and sympathetic neuropathies in mice carrying a disrupted Trk/NGF receptor gene. *Nature* 1994; 368: 246–249.
18. Davis BM, Lewin GR, Mendell LM, Jones ME and Albers KM. Altered expression of nerve growth factor in the skin of transgenic mice leads to changes in response to mechanical stimuli. *Neuroscience* 1993; 56: 789–792.
19. Stucky CL, Koltzenburg M, Schneider M, Engle MG, Albers KM and Davis BM. Overexpression of nerve growth factor in skin selectively affects the survival and functional properties of nociceptors. *J Neurosci* 1999; 19: 8509–8516.
20. Mantyh WG, Jimenez-Andrade JM, Stake JI, Bloom AP, Kaczmarska MJ, Taylor RN, Freeman KT, Ghilardi JR, Kuskowski MA and Mantyh PW. Blockade of nerve sprouting and neuroma formation markedly attenuates the development of late stage cancer pain. *Neuroscience* 2010; 171: 588–598.
21. Halvorson KG. A blocking antibody to nerve growth factor attenuates skeletal pain induced by prostate tumour cells growing in bone. *Cancer Res* 2005; 65: 9426–9435.
22. Jimenez-Andrade JM, Bloom AP, Stake JI, Mantyh WG, Taylor RN, Freeman KT, Freeman KT, Ghilardi JR, Kuskowski MA and Mantyh PW. Pathological sprouting of adult nociceptors in chronic prostate cancer-induced bone pain. *J Neurosci* 2010; 30: 14649–14656.
23. Sevcik MA, Ghilardi JR, Peters CM, Lindsay TH, Halvorson KG, Jonas BM, Kubota K, Kuskowski MA, Boustany L, Shelton DL and Mantyh PW. Anti-NGF therapy profoundly reduces bone cancer pain and the accompanying increase in markers of peripheral and central sensitization. *Pain* 2005; 115: 128–141.
24. Jimenez-Andrade JM, Martin CD, Koewler NJ, Freeman KT, Sullivan LJ, Halvorson KG, Barthold CM, Peters CM, Buus RJ, Ghilardi JR, Lewis JL, Kuskowski MA and Mantyh PW. Nerve growth factor sequestering therapy attenuates non-malignant skeletal pain following fracture. *Pain* 2007; 133: 183–196.
25. McNamee KE, Burleigh A, Gompels LL, Feldmann M, Allen SJ, Williams RO, Dawbarn D, Vincent TL and Inglis JJ. Treatment of murine osteoarthritis with TrkAd5 reveals a pivotal role for nerve growth factor in non-inflammatory joint pain. *Pain* 2010; 149: 386–392.
26. Castañeda-Corral G, Jimenez-Andrade JM, Bloom AP, Taylor RN, Mantyh WG, Kaczmarska MJ, Ghilardi JR and Mantyh PW. The majority of myelinated and unmyelinated sensory nerve fibers that innervate bone express the tropomyosin receptor kinase A. *Neuroscience* 2011; 178: 196–207.
27. Bloom AP, Jimenez-Andrade JM, Taylor RN, Castañeda-Corral G, Kaczmarska MJ, Freeman KT, Coughlin KA, Ghilardi JR, Kuskowski MA and Mantyh PW. Breast cancer-induced bone remodeling, skeletal pain, and sprouting of sensory nerve fibers. *J. Pain* 2011; 12: 698–711.
28. Mantyh PW, Koltzenburg M, Mendell LM, Tive L and Shelton DL. Antagonism of nerve growth factor-TrkA signaling and the relief of pain. *Anesthesiology* 2011; 115: 189–204.

29. Taylor S, Srinivasan B, Wordinger RJ and Roque RS. Glutamate stimulates neurotrophin expression in cultured Müller cells. *Brain Res Mol Brain Res* 2003; 111: 189–197.
30. Xiong H, Futamura T, Jourdi H, Zhou H, Takei N, Diverse-Pierluissi M, Plevy S and Nawa H. Neurotrophins induce BDNF expression through the glutamate receptor pathway in neocortical neurons. *Neuropharmacology* 2002; 42: 903–912.
31. Liu X, Resch J, Rush T and Lobner D. Functional upregulation of system xc^- by fibroblast growth factor-2. *Neuropharmacology* 2012; 62: 901–906.
32. Shih AY, Erb H, Sun X, Toda S, Kalivas PW and Murphy TH. Cystine/glutamate exchange modulates glutathione supply for neuroprotection from oxidative stress and cell proliferation. *J Neurosci* 2006; 26: 10514–10523.
33. Lagadec C, Meignan S, Adriaenssens E, Foveau B, Vanhecke E, Romon R, Toillon R-A, Oxombre B, Hondermarck H and Le Bourhis X. TrkA overexpression enhances growth and metastasis of breast cancer cells. *Oncogene* 2009; 28: 1960–1970.
34. Ohmichi M, Pang L, Ribon V, Gazit A, Levitzki A and Saltiel AR. The tyrosine kinase inhibitor tyrphostin blocks the cellular actions of nerve growth factor. *Biochemistry* 1993; 32: 4650–4658.
35. Linher-Melville K, Nashed MG, Ungard RG, Haftchenary S, Rosa DA, Gunning PT and Singh G. Chronic inhibition of STAT3/STAT5 in treatment-resistant human breast cancer cell subtypes: convergence on the ROS/SUMO pathway and its effects on xCT expression and system xc^- activity. *PLoS One* 2016; 11: e0161202.
36. Lutgen V, Qualmann K, Resch J, Kong L, Choi S and Baker DA. Reduction in phencyclidine induced sensorimotor gating deficits in the rat following increased system xc^- activity in the medial prefrontal cortex. *Psychopharmacology* 2013; 226: 531–540.
37. Chenu C. Glutamatergic regulation of bone remodeling. *J Musculoskelet Neuronal Interact* 2002; 2: 282–284.
38. Luger NM, Honore P, Sabino MA, Schwei MJ, Rogers SD, Mach DB, Clohisy DR and Mantyh PW. Osteoprotegerin diminishes advanced bone cancer pain. *Cancer Res* 2001; 61: 4038–4047.
39. Robinson I, Sargent B and Hatcher JP. Use of dynamic weight bearing as a novel end-point for the assessment of Freund's Complete Adjuvant induced hypersensitivity in mice. *Neurosci Lett* 2012; 524: 107–110.
40. Nirogi R, Goura V, Shanmuganathan D, Jayarajan P and Abraham R. Comparison of manual and automated filaments for evaluation of neuropathic pain behavior in rats. *J Pharmacol Toxicol Methods* 2012; 66: 8–13.
41. Pulaski BA and Ostrand-Rosenberg S. Mouse 4T1 breast tumour model. *Curr Protoc Immunol* Chapter 20: Unit 20.2. Epub ahead of print May 2001. DOI: 10.1002/0471142735.im2002s39.
42. De Ciantis PD, Yashpal K, Henry J and Singh G. Characterization of a rat model of metastatic prostate cancer bone pain. *J Pain Res* 2010; 3: 213.
43. Lozano-Ondoua AN, Symons-Liguori AM and Vanderah TW. Cancer-induced bone pain: Mechanisms and models. *Neurosci Lett* 2013; 557 Pt A: 52–59.
44. Breese NM, George AC, Pauers LE and Stucky CL. Peripheral inflammation selectively increases TRPV1 function in IB4-positive sensory neurons from adult mouse. *Pain* 2005; 115: 37–49.
45. Asai H, Ozaki N, Shinoda M, Nagamine K, Tohnai I, Ueda M and Sugiura Y. Heat and mechanical hyperalgesia in mice model of cancer pain. *Pain* 2005; 117: 19–29.
46. Inoue M, Rashid MH, Fujita R, Contos JJA, Chun J and Ueda H. Initiation of neuropathic pain requires lysophosphatidic acid receptor signaling. *Nat Med* 2004; 10: 712–718.
47. Seidlitz EP, Sharma MK and Singh G. Extracellular glutamate alters mature osteoclast and osteoblast functions. *Can J Physiol Pharmacol* 2010; 88: 929–936.
48. Jimenez-Andrade JM, Ghilardi JR, Castañeda-Corral G, Kuskowski MA and Mantyh PW. Preventive or late administration of anti-NGF therapy attenuates tumour-induced nerve sprouting, neuroma formation, and cancer pain. *Pain* 2011; 152: 2564–2574.
49. Larsson L-I. Novel actions of tyrphostin AG 879: inhibition of RAF-1 and HER-2 expression combined with strong antitumoural effects on breast cancer cells. *Cell Mol Life Sci* 2004; 61: 2624–2631.
50. Huang EJ and Reichardt LF. Trk receptors: roles in neuronal signal transduction. *Annu Rev Biochem* 2003; 72: 609–642.
51. Linher-Melville K, Haftchenary S, Gunning P and Singh G. Signal transducer and activator of transcription 3 and 5 regulate system Xc^- and redox balance in human breast cancer cells. *Mol Cell Biochem* 2015; 405: 205–221.
52. Linher-Melville K and Singh G. The complex roles of STAT3 and STAT5 in maintaining redox balance: Lessons from STAT-mediated xCT expression in cancer cells. *Mol Cell Endocrinol* 2017; 451:40–52.
53. Skerry TM. The role of glutamate in the regulation of bone mass and architecture. *J Musculoskelet Neuronal Interact* 2008; 8: 166–173.
54. Takarada T and Yoneda Y. Pharmacological topics of bone metabolism: glutamate as a signal mediator in bone. *J Pharmacol Sci* 2008; 106: 536–541.
55. Merle B, Itzstein C, Delmas PD and Chenu C. NMDA glutamate receptors are expressed by osteoclast precursors and involved in the regulation of osteoclastogenesis. *J Cell Biochem* 2003; 90: 424–436.
56. Peet NM, Grabowski PS, Laketic-Ljubojevic I and Skerry TM. The glutamate receptor antagonist MK801 modulates bone resorption in vitro by a mechanism predominantly involving osteoclast differentiation. *FASEB J* 1999; 13: 2179–2185.
57. Itzstein C, Espinosa L, Delmas PD and Chenu C. Specific antagonists of NMDA receptors prevent osteoclast sealing zone formation required for bone resorption. *Biochem Biophys Res Commun* 2000; 268: 201–209.
58. Taylor AF. Osteoblastic glutamate receptor function regulates bone formation and resorption. *J Musculoskelet Neuronal Interact* 2002; 2: 285–290.
59. Rose AAN and Siegel PM. Breast cancer-derived factors facilitate osteolytic bone metastasis. *Bull Cancer* 2006; 93: 931–943.

60. Coleman RE, Lipton A, Roodman GD, Guise TA, Boyce BF, Brufsky AM, Clézardin P, Croucher PI, Gralow JR, Hadji P, Holen I, Mundy GR, Smith MR and Suva LJ. Metastasis and bone loss: advancing treatment and prevention. *Cancer Treat Rev* 2010; 36: 615–620.
61. Boyle WJ, Simonet WS and Lacey DL. Osteoclast differentiation and activation. *Nature* 2003; 423: 337–342.
62. Dougall WC and Chaisson M. The RANK/RANKL/OPG triad in cancer-induced bone diseases. *Cancer Metastasis Rev* 2006; 25: 541–549.
63. Wang L, Hinoi E, Takemori A, Nakamichi N and Yoneda Y. Glutamate inhibits chondral mineralization through apoptotic cell death mediated by retrograde operation of the cystine/glutamate antiporter. *J Biol Chem* 2006; 281: 24553–24565.